

## Discovery of Macrocyclic Hydroxamic Acids Containing Biphenylmethyl Derivatives at P1', a Series of Selective TNF- $\alpha$ Converting Enzyme Inhibitors with Potent Cellular Activity in the Inhibition of TNF- $\alpha$ Release

Chu-Biao Xue,\* Xiaohua He, Ronald L. Corbett, John Roderick, Zelda R. Wasserman, Rui-Qin Liu, Bruce D. Jaffee,<sup>†</sup> Maryanne B. Covington, Mingxin Qian, James M. Trzaskos, Robert C. Newton, Ronald L. Magolda,<sup>‡</sup> Ruth R. Wexler, and Carl P. Decicco\*

DuPont Pharmaceuticals Company, Experimental Station,  
P.O. Box 80500, Wilmington, Delaware 19880-0500

Received July 5, 2001

**Abstract:** SAR exploration at P1' using an *anti*-succinate-based macrocyclic hydroxamic acid as a template led to the identification of several bulky biphenylmethyl P1' derivatives which confer potent porcine TACE and anti-TNF- $\alpha$  cellular activities with high selectivity versus most of the MMPs screened. Our studies demonstrate for the first time that TACE has a larger S1' pocket in comparison to MMPs and that potent and selective TACE inhibitors can be achieved by incorporation of sterically bulky P1' residues.

Tumor necrosis factor  $\alpha$  (TNF- $\alpha$ ),<sup>1</sup> a proinflammatory cytokine, is a key mediator of the biological response to bacterial infection and inflammation and an inducer of other proinflammatory cytokines such as IL-1 $\beta$ , IL-6, and IL-8. In response to a variety of stimuli, TNF- $\alpha$  is synthesized primarily by activated monocytes/macrophages as a 233-amino acid membrane-bound precursor. The pro-TNF- $\alpha$  is then processed by a metalloproteinase called TNF- $\alpha$  converting enzyme (TACE)<sup>2,3</sup> to release a soluble form of TNF- $\alpha$  comprising 157 amino acids, which exerts its biological functions via interaction with two structurally and functionally distinct high-affinity receptors: TNFR1 (p55) and TNFR2 (p75). During normal host defense, low levels of serum TNF- $\alpha$  confer protection against infectious agents, tumors, and tissue damage and have an important role in the development of the humoral immune response. However, overproduction of TNF- $\alpha$  is associated with symptoms of a variety of infectious, autoimmune, and inflammatory disorders including rheumatoid arthritis (RA) and Crohn's disease.<sup>4</sup>

The central role of TNF- $\alpha$  in autoimmune diseases has been clearly demonstrated by the benefit in treating Crohn's disease and RA using the monoclonal TNF- $\alpha$  antibody, Remicade (infliximab),<sup>5</sup> and the soluble TNF p75 receptor fusion protein (TNFRp75:Fc), Enbrel (etanercept).<sup>6</sup> These recently approved biologics eliminate TNF- $\alpha$  effects by neutralizing excess TNF- $\alpha$  and have proven to be effective anti-TNF- $\alpha$  therapeutics. As

proteins, however, these drugs are expensive and inconvenient to patients. Given these drawbacks, small molecule anti-TNF- $\alpha$  agents are currently being exploited through multiple approaches. One very promising approach is the inhibition of TNF- $\alpha$  processing through the inhibition of TACE.

TACE (ADAM 17) is a membrane anchored multidomain enzyme containing extracellular disintegrin and protease regions. It has been shown that TACE is the primary enzyme responsible for the processing of the biologically active soluble TNF- $\alpha$  from its membrane-bound proform, and inhibition of TACE blocks TNF- $\alpha$  release.<sup>7</sup> This experimental evidence strongly implicates the therapeutic potential of TACE inhibitors for the treatment of TNF- $\alpha$  mediated pathologies. As a result, TACE has recently emerged as an important therapeutic target.<sup>8</sup>

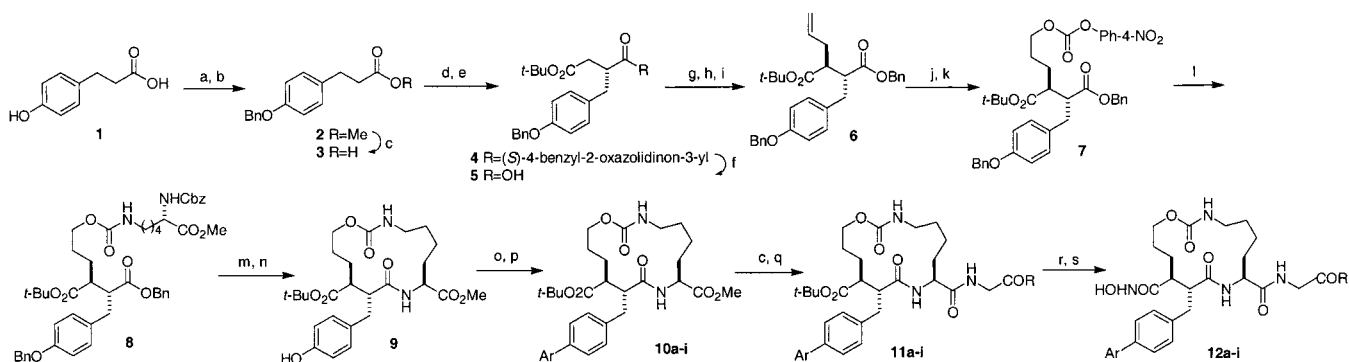
As a member of the adamalysin/ADAM subfamily of the metzincin superfamily that also includes the astacins, serralysins, and metalloproteinases (MMPs), TACE shows relatively low overall sequence homology to MMPs but has significant similarity in the active site as revealed by its X-ray crystal structure.<sup>9</sup> Not surprisingly, some broad-spectrum MMP inhibitors have been shown to be capable of inhibiting TNF- $\alpha$  processing.<sup>10,11</sup> While this crossover in TACE activity of the extensively explored MMP inhibitors<sup>12</sup> offers advantages in lead identification of small molecule TACE inhibitors, it also creates some difficulty in further optimization to achieve TACE selectivity. Selective TACE inhibitors are needed to clearly delineate the centrality of this target for the specific inhibition of TNF- $\alpha$  and the role of TACE in cell surface protein shedding. Moreover, selective TACE inhibitors are desirable in the long-term treatment of TNF- $\alpha$  mediated pathologies since inhibition of multiple MMPs may lead to unwanted toxicity. For example, broad-spectrum MMP inhibitors have been found to cause side-effects in oncology clinical trials,<sup>13</sup> which may be attributed to the nonspecific inhibition of MMPs required for normal physiological matrix turnover.

We have previously reported the design, synthesis, and structure–activity relationships of a new class of macrocyclic hydroxamic acids that are potent TACE inhibitors and broad spectrum MMP inhibitors as well.<sup>14</sup> In an attempt to eliminate the MMP activity from this class of TACE inhibitors, we selected SP057 as a template for SAR exploration in the P1' position. SP057, a 15-membered cyclic carbamate with an isobutyl at P1' and a glycine 4-morpholinylamide at P3'–P4', is the most potent inhibitor reported in the literature to date for the inhibition of TNF- $\alpha$  release from LPS-stimulated human whole blood, with an IC<sub>50</sub> of 67 nM.<sup>14</sup> Our primary goal was to achieve >100-fold TACE selectivity over most of the MMPs while maintaining the whole blood potency of SP057. On the basis of a homology model of TACE<sup>15</sup> and the availability of starting materials, we elected to replace the P1' isobutyl in SP057 with 4-hydroxybenzyl, the hydroxyl of which was then used as a handle to introduce a variety of substituted aryl residues via Suzuki coupling to form biphenylmethyl derivatives at P1'.<sup>16</sup>

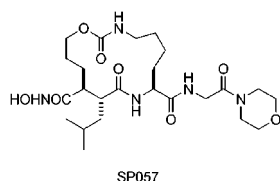
\* Corresponding author: Chu-Biao Xue. Phone: 302-695-2053. Fax 302-695-1173. E-mail: chu-biao.xue@dupontpharma.com.

<sup>†</sup> Current address: Millenium Pharmaceuticals, 215 First Street, Cambridge, MA 02142.

<sup>‡</sup> Current address: Boehringer-Ingelheim, 900 Ridgebury Road, P.O. Box 368, Ridgefield, CT 06877-0368.

Scheme 1<sup>a</sup>

<sup>a</sup> Conditions: (a) 4 N HCl/dioxane, MeOH, 100%; (b) BnBr, K<sub>2</sub>CO<sub>3</sub>, DMF, 80 °C, 90%; (c) LiOH, THF, 98%; (d) pivaloyl chloride, DIEA, LiCl, (S)-4-benzyl-2-oxazolidinone, THF, 60%; (e) *tert*-butyl bromoacetate, LDA, THF, 59%; (f) LiOH, H<sub>2</sub>O<sub>2</sub>, THF, 100%; (g) allyl bromide, 2.1 × LDA, THF, 84%; (h) 2.1 × LDA, Et<sub>2</sub>AlCl, THF, MeOH; (i) BnBr, DBU, benzene, reflux, 88%; (j) 9-BBN, THF, NaOAc, H<sub>2</sub>O<sub>2</sub>, 87%; (k) 4-nitrophenyl chloroformate, DIEA, THF, 78%; (l) *N*<sup>ε</sup>-Cbz-L-LysOMe, K<sub>2</sub>CO<sub>3</sub>, DMF, 81%; (m) H<sub>2</sub>, Pd-C, MeOH, 93%; (n) BOP, DIEA, CHCl<sub>3</sub>, 94%; (o) PhN(Tf)<sub>2</sub>, NEt<sub>3</sub>, CH<sub>2</sub>Cl<sub>2</sub>; (p) ArB(OH)<sub>2</sub>, Pd(PPh<sub>3</sub>)<sub>4</sub>, KBr, K<sub>2</sub>CO<sub>3</sub>, DMF, H<sub>2</sub>O; (q) GlyR, BOP, DIEA, DMF; (r) TFA, CH<sub>2</sub>Cl<sub>2</sub>; (s) HONH<sub>2</sub>·HCl, BOP, DIEA, DMF.

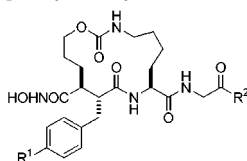


**Synthesis.** The macrocycles of the present study were prepared using the protocol outlined in Scheme 1. Esterification of 3-(4-hydroxyphenyl)propionic acid **1** followed by benzylation at the phenolic OH provided the ester **2**. Following hydrolysis of **2** using LiOH, the carboxylic acid **3** was coupled with the chiral auxiliary group (S)-4-benzyl-2-oxazolidinone, and the resulting intermediate was subjected to an LDA-promoted diastereoselective alkylation with *tert*-butyl bromoacetate. After removal of the chiral auxiliary group in **4** using LiOH/H<sub>2</sub>O<sub>2</sub>, dianion alkylation of the resulting carboxylic acid **5** with allyl bromide followed by epimerization and benzylation produced the *anti*-succinate derivative **6**. The olefin in **6** was converted to an alcohol by treatment with 9-BBN, and the resulting alcohol was subjected to a reaction with 4-nitrophenyl chloroformate to provide the activated carbonate **7**, which was reacted with *N*<sup>ε</sup>-Cbz-L-LysOMe to afford the carbamate **8**. Catalytic hydrogenolysis of **8** followed by intramolecular cyclization using BOP furnished the cyclic carbamate **9**. Conversion of the phenolic OH in **9** to a triflate and Suzuki coupling of the triflate with an aryl boronic acid provided the biphenyl derivatives **10a–i**. Saponification of the methyl ester using LiOH followed by coupling of the resulting carboxylic acid with a glycine amide gave rise to the intermediates **11a–i**. The hydroxamic acids **12a–i** were then obtained by treatment of **11a–i** with TFA followed by coupling of the resulting carboxylic acid with hydroxylamine using BOP.

**Results and Discussion.** TACE activities were assessed using a porcine TACE (pTACE) assay. All compounds were counterscreened with MMP-1, MMP-2, and MMP-9 assays. Cellular activities were determined using an LPS-stimulated human whole blood assay (WBA).<sup>17</sup> As shown in Table 1, replacement of the isobutyl P1' in SP057 with 4-(2,6-difluorophenyl)benzyl, 4-(3,5-dichlorophenyl)benzyl, 4-(2-methylsulfonylphenyl)benzyl, and 4-(2-trifluoromethylphenyl)benzyl af-

forded analogues **12a–d**, which exhibited pTACE activity similar to SP057. Although analogues **12a–b** were devoid of MMP-1 activity, they displayed good potency in the inhibition of MMP-2 and MMP-9. This is consistent with the previous observations that MMP-1 has a small S1' pocket whose depth is defined by the side chain of Arg-214 at the bottom of the pocket,<sup>18</sup> whereas MMP-2 and MMP-9 have relatively deeper and larger S1' pockets.<sup>19,20</sup> Analogues **12c–d**, however, were totally inactive against MMP-1, MMP-2, and MMP-9, demonstrating high TACE selectivity over the three MMPs screened. Equally important to its TACE selectivity, analogue **12d** exhibited a cellular activity equipotent to the nonselective inhibitor SP057, with an IC<sub>50</sub> of 70 nM in WBA. Comparison of pTACE activity and WBA potency among analogues **12a–d** revealed that the substituent(s) on the distal phenyl ring had little effect on pTACE activity but significantly affected cellular potency. Human serum protein binding studies indicate that the dramatic changes in cellular potency among these four analogues are not caused by changes in protein binding. For instance, despite its higher protein binding, analogue **12d** displayed WBA potency 52 and 6 times better than analogues **12a** and **12c**, respectively. It is likely that cell penetration may play an important role in WBA potency. The 4-(2-trifluoromethylphenyl)benzyl P1' residue of **12d** appears to manifest better cell penetration than the 4-(2,6-difluorophenyl)benzyl (**12a**) and the 4-(2-methylsulfonylphenyl)benzyl residues (**12c**). Since analogue **12d** has higher protein binding than SP057, it is also likely that the P1' substituent of **12d** may facilitate better cell penetration than the isobutyl group of SP057, compensating for its higher protein binding and resulting in similar cellular potency between the two molecules.

Keeping the 4-(2-trifluoromethylphenyl)benzyl residue at P1' constant, we examined three other P4' substituents as shown in **12e–g**. Apart from the P4' piperazin-1-yl analogue **12g**, which exhibited a profile comparable to **12d**, the other two analogues **12e** and **12f** offered no advantage over **12d** in terms of cellular activity and/or TACE selectivity. The slight loss in TACE selectivity observed for **12f** may be attributed to extra binding interaction with MMP-2 and MMP-9 in

**Table 1.** Macrocyclic Hydroxamic Acids Containing Biphenylmethyl Derivatives at P1'

cpd	R <sup>1</sup>	R <sup>2</sup>	pTACE <sup>a</sup> K <sub>i</sub> , nM	WBA <sup>b</sup> IC <sub>50</sub> , nM	K <sub>i</sub> , nM <sup>a</sup>			PB <sup>c</sup> % bound
					MMP-1	MMP-2	MMP-9	
SP057			4.2	67	13	1.1	1.2	1
<b>12a</b>	2,6-difluorophenyl	morpholin-4-yl	6.3	3700	>2000	0.64	21	25
<b>12b</b>	3,5-dichlorophenyl	morpholin-4-yl	2.8	227	>2000	50	183	83
<b>12c</b>	2-(methylsulfonyl)phenyl	morpholin-4-yl	6.5	410	>2000	>2000	>2000	5
<b>12d</b>	2-(trifluoromethyl)phenyl	morpholin-4-yl	2.8	70	>2000	>2000	>2000	55
<b>12e</b>	2-(trifluoromethyl)phenyl	NH <sub>2</sub>	1.5	180	>2000	1867	>2000	NT <sup>d</sup>
<b>12f</b>	2-(trifluoromethyl)phenyl	NHMe	3.8	380	>2000	450	1170	33
<b>12g</b>	2-(trifluoromethyl)phenyl	piperazin-1-yl	1.7	60	>2000	700	1787	36
<b>12h</b>	3-(trifluoromethyl)phenyl	piperazin-1-yl	3.7	120	>2000	11	91	29
<b>12i</b>	3,5-(bistrifluoromethyl)phenyl	piperazin-1-yl	4.6	180	>2000	>2000	>2000	71

<sup>a</sup> K<sub>i</sub> values are from three determinations. <sup>b</sup> Inhibition of TNF-α release in LPS-stimulated human whole blood assay (WBA) was determined in three donors. <sup>c</sup> Human serum protein binding (PB) is given as mean percentage bound from three determinations. <sup>d</sup> NT = not tested.

**Table 2.** Inhibitory Profiles for Compounds **12d**, **12e**, **12g**, and **12i**

enzyme	<b>12d</b> K <sub>i</sub> , nM	<b>12e</b> K <sub>i</sub> , nM	<b>12g</b> K <sub>i</sub> , nM	<b>12i</b> K <sub>i</sub> , nM
pTACE	2.8	1.5	1.5	4.6
MMP-1	>2000	>2000	>2000	>2000
MMP-2	>2000	1867	700	>2000
MMP-3	>2000	>2000	582	>2000
MMP-7	834	1336	177	>2000
MMP-8	126	428	672	272
MMP-9	>2000	>2000	1787	>2000
MMP-10	>2000	>2000	>2000	>2000
MMP-12	>2000	>2000	390	35
MMP-13	653	442	50	>2000
MMP-14	>2000	>2000	>2000	>2000
MMP-15	>2000	>2000	>2000	>2000
MMP-16	>2000	>2000	>2000	>2000

the P4' position. Surprisingly, moving the trifluoromethyl group on the distal phenyl ring from 2-position in **12g** to the 3-position (**12h**) abolishes TACE selectivity over MMP-2 and MMP-9. However, introduction of a second trifluoromethyl group at the 5-position in **12h** provided another very selective analogue **12i**, which was approximately 2-fold less active than the two most attractive inhibitors **12d** and **12g** in WBA.

To get an insight into the selectivity profile over other MMPs, analogues **12d**, **12e**, **12g**, and **12i** were screened against a panel of twelve MMPs. As shown in Table 2, all these analogues exhibited >100-fold TACE selectivity over MMP-1, MMP-2, MMP-3, MMP-7, MMP-9, MMP-10, MMP-14, MMP-15, and MMP-16. Slightly less selectivity was observed for **12d** and **12i** over MMP-8, **12g** over MMP-13, and **12i** over MMP-12.

To address the difference in binding at the S1' subsites between TACE and MMPs, analogues **12g–i** were docked into the crystal structure of MMP-2 and a model of the active site of TACE which had been built based on homology to atrolysin (Figure 1). In the S1' pocket of MMP-2, the 2-trifluoromethyl substituent of analogue **12g**, in which the two phenyl rings of the biphenyl moiety would adopt a nearly orthogonal orientation with high barriers to ring rotation, seems to have an unfavorable interaction with the side chain of a tyrosine residue which is conserved in all MMPs.<sup>21</sup>

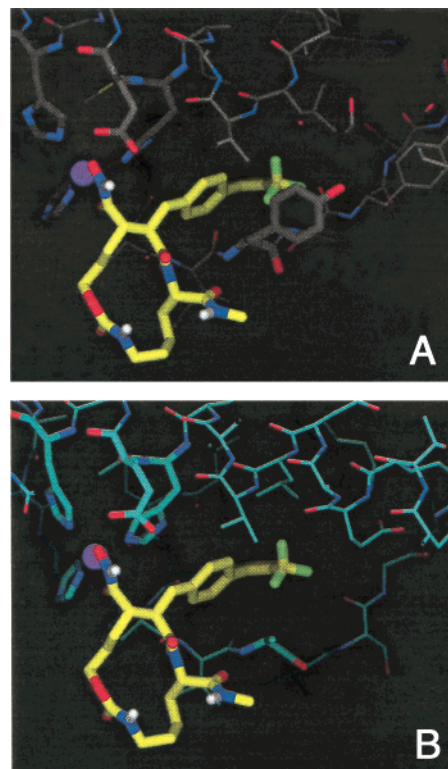


**Figure 1.** Docking of compound **12g** into the active site of MMP-2 (A) and a model of TACE (B) which was built from homology to atrolysin (see ref 15). In both pictures (A and B), inhibitor **12g** is shown with P4' truncated. In the S1' pockets, the tyrosine residue of MMP-2 is replaced by an alanine residue in TACE, causing the difference in inhibitory activity between MMP-2 and TACE.

This bulky substituent also would not be well-accommodated in the opposite side of the pocket which is a tight area as well. Although the biphenyl moiety can be turned around by rotation around the bond between the biphenyl and methylene residues, this rotation would give rise to a geometry unsuited for the shape of the S1' pocket. In contrast, the 3-substitution in analogue **12h** orients the trifluoromethyl group to the rear of the tyrosine side chain, resulting in little steric repulsion. In addition, the bond connecting the two

phenyl rings of the biphenyl moiety in **12h** can rotate more freely, allowing the P1' side chain to adjust to the shape of the S1' pocket without requiring much energy. These observations probably account for the difference in MMP-2 activity between **12g** and **12h**. The 4-(3,5-bistrifluoromethylphenyl)benzyl residue in **12i** seems too bulky to fit into the MMP-2 S1' subsite. In the S1' pocket of TACE, replacement of the MMP-conserved Tyr residue, which forms the outer wall of the S1' region, by an alanine residue removes the steric interaction with the 2-trifluoromethyl residue on the distal phenyl in **12g**. Moreover, according to our model, the shape of the TACE S1' pocket is different from that of MMP-2, providing a suitable room for the easy accommodation of all the P1' substituents in **12g-i**.

**Conclusion.** Using an *anti*-succinate-based macrocyclic hydroxamic acid (SP057) as a template, several biphenylmethyl derivatives were examined at P1'. Among them, 4-(2-methylsulfonylphenyl)benzyl, 4-(2-trifluoromethylphenyl)benzyl, and 4-(3,5-bistrifluoromethylphenyl)benzyl residues were identified to confer potent pTACE activity with high selectivity versus MMP-1, MMP-2, and MMP-9. Further profiling for three 4-(2-trifluoromethylphenyl)benzyl P1' analogues (**12d**, **12e**, and **12g**) and the 4-(3,5-bistrifluoromethylphenyl)benzyl P1' analogue (**12i**) revealed that these bulky P1' analogues are also selective over most of other MMPs screened. The high selectivity of these TACE inhibitors probably stems from replacement of the MMP-conserved Tyr residue by an Ala residue in TACE and the shape difference between TACE and MMPs at the S1' subsites. Equally important to their TACE selectivity, these compounds are potent in the inhibition of TNF- $\alpha$  release from LPS-stimulated human whole blood. A combination of 4-(2-trifluoromethylphenyl)benzyl at P1' and glycine 4-morpholinylamide or glycine 1-piperazinylamide at P3'-P4' afforded two attractive TACE inhibitors **12d** and **12g** which exhibited >100-fold selectivity over a panel of 11 MMPs and a cellular activity equipotent to SP057 in WBA (IC<sub>50</sub> values of 70 and 60 nM, respectively). Our studies demonstrate that TACE has a larger S1' pocket in comparison to MMPs, and that selective and potent TACE inhibitors can be achieved by incorporation of appropriate sterically bulky P1' residues.

**Acknowledgment.** We thank Sherrill A. Nurnberg, Dianna L. Blessington, Persymphonie B. Miller, Theresa M. Dimeo, John Giannaras, Robert J. Collins, Tracy L. Taylor, and Paul J. Strzemienski for performing pTACE, MMP, and whole blood assays.

**Supporting Information Available:** Experimental details for the syntheses of compounds **12a-i** and their spectroscopic data. This material is available free of charge via the Internet at <http://pubs.acs.org>.

## References

- (1) Aggarwal, B.; Kohr, W.; Hass, P.; et al. Human tumour necrosis factor: Production, purification and characterization. *J. Biol. Chem.* **1985**, *260*, 2345-2354.
- (2) Black, R.; Rauch, C.; Kozlosky, C.; et al. A metalloproteinase disintegrin that releases tumour necrosis factor- $\alpha$  from cells. *Nature* **1997**, *385*, 729-733.
- (3) Moss, M.; Jin, S.-L.; Milla, M.; et al. Cloning of a disintegrin metalloproteinase that processes precursor tumour-necrosis factor- $\alpha$ . *Nature* **1997**, *385*, 733-736.
- (4) Eigler, A.; Sinha, B.; Hartmann, G.; Endres, S. Taming TNF: strategies to restrain this proinflammatory cytokine. *Immunol. Today* **1997**, *18*, 487-492.
- (5) Elliott, M.; Maini, R.; Feldmann, M.; et al. Repeated therapy with monoclonal antibody to tumour necrosis factor  $\alpha$  (cA2) in patients with rheumatoid arthritis. *Lancet* **1994**, *344*, 1125-1127.
- (6) Moreland, L.; Baumgartner, S.; Schiff, M.; et al. Treatment of rheumatoid arthritis with a recombinant human tumor necrosis factor receptor (p75)-Fc fusion protein. *N. Engl. J. Med.* **1997**, *337*, 141-147.
- (7) Mohler, K.; Sleath, P.; Fitzner, J.; et al. Protection against a lethal dose of endotoxin by an inhibitor of tumour necrosis factor processing. *Nature* **1994**, *370*, 218-220.
- (8) Nelson, F.; Zask, A. The therapeutic potential of small molecule TACE inhibitors. *Expert Opin. Invest. Drugs* **1999**, *8*, 383-392.
- (9) Maskos, K.; Fernandez-Catalan, C.; Huber, R.; et al. Crystal structure of the catalytic domain of human tumor necrosis factor- $\alpha$ -converting enzyme. *Proc. Natl. Acad. Sci. U.S.A.* **1998**, *95*, 3408-3412.
- (10) McGeehan, G.; Becherer, J.; Bast, R., Jr.; et al. Regulation of tumour necrosis factor- $\alpha$  by a metalloproteinase inhibitor. *Nature* **1994**, *370*, 558-561.
- (11) Gearing, A.; Beckett, P.; Christodoulou, M.; et al. Processing of tumour necrosis factor- $\alpha$  precursor by metalloproteinases. *Nature* **1994**, *370*, 555-557.
- (12) Michaelides, M.; Curtin, M. Recent advances in matrix metalloproteinase inhibitors research. *Curr. Pharm. Des.* **1999**, *5*, 787-819.
- (13) Rothenberg, M.; Nelson, A.; Hande, K. New drugs on the horizon: matrix metalloproteinase inhibitors. *Oncologist* **1998**, *3*, 271-274.
- (14) Xue, C.-B.; Voss, M.; Nelson, D.; et al. Design, synthesis and structure-activity relationships of macrocyclic hydroxamic acids that inhibit TNF- $\alpha$  release in vitro and in vivo. *J. Med. Chem.* **2001**, *44*, 2636-2660.
- (15) A homology model of TACE was built based on the crystal structure of atrolysin. Comparison of the model with crystal structures of MMPs revealed differences in shape and size of S1' pockets. For example, the S1' pocket of MMP-1 is foreshortened by an arginine (Arg-214) side chain, that of MMP-8 by another arginine 6 or 7 Å deeper into the pocket, and that of MMP-3 extends straight back from the protein surface. In contrast, the S1' pocket of the TACE model is spacious, exhibiting a curved or boomerang-like shape.
- (16) Biphenylethyl residues have been employed as P1' substituents in carboxyalkyl dipeptides to provide a series of potent MMP-2 and MMP-3 inhibitors (see ref 19).
- (17) TACE, MMP, and LPS-stimulated human whole blood assays were performed using the protocols described in ref 19.
- (18) Lovejoy, B.; Welch, A.; Carr, S.; et al. Crystal structure of MMP-1 and -13 reveal the structural basis for selectivity of collagenase inhibitors. *Nature Struct. Biol.* **1999**, *6*, 217-221.
- (19) Esser, C.; Bugianesi, R.; Caldwell, C.; et al. Inhibition of stromelysin (MMP-3) by P1'-biphenylethyl carboxyalkyl dipeptides. *J. Med. Chem.* **1997**, *40*, 1026-1040.
- (20) Kiyama, R.; Tamura, Y.; Watanabe, F.; et al. Homology modeling of gelatinase catalytic domains and docking simulations of novel sulfonamide inhibitors. *J. Med. Chem.* **1999**, *42*, 1723-1738.
- (21) The numbering of the tyrosine residue in the S1' subsites of MMPs is different from one enzyme to another. For example, the residue numbers are Tyr-240 in MMP-1 and Tyr-223 in MMP-3.

JM0155502